ChemPubSoc Europe

DOI: 10.1002/cctc.201801193

CHEMCATCHEM Full Papers

Study of the Electroreactivity of Amoxicillin on Carbon Nanotube-Supported Metal Electrodes

Marta Ferreira,[a] Iwona Kuzniarska-Biernacka,[a] António M. Fonseca,[a, b] Isabel C. Neves,[a, b] Olívia S. G. P. Soares,[c] Manuel F. R. Pereira,[c] José L. Figueiredo,[c] and Pier Parpot*[a, b]

The electroreactivity of amoxicillin (AMX) was studied on catalysts based on platinum, palladium and ruthenium supported on carbon nanotubes (Pt/CNT, Pd/CNT, Ru/CNT) in aqueous media using cyclic voltammetry. Cyclic voltammograms show two oxidation processes, the first one between 0.5 and 1.0 V *vs.* reference hydrogen electrode (RHE) and the second one between 1.2 and 1.6 V *vs.* RHE. The effects of electrocatalytic material and supporting electrolyte, on current intensities and oxidation potentials, were determined using experimental design strategy (DOE). Kinetic parameters of the oxidation reactions were calculated from the scan rate study. The constant potential electrolysis of AMX was carried out on Ru/CNT catalyst, in 0.1 M NaOH and AMX conversion reached 45% after 6 h of electrolysis at 2.5 V *vs.* RHE. The percentages of CO_3^{2-}, SO_4^{2-} and NO_3^- among oxidation products were 26, 17 and 4%, respectively. The primary degradation products of AMX determined by HPLC-MS gave some insight about the reaction pathways.

Introduction

The presence of pharmaceutical compounds, especially antibiotics in water and wastewater is increasing the concern related to the environmental contamination since the conventional biological treatments seem to be unsatisfactory in this case. Due to their potential risk, recently an important number of scientific works in the field of the detection of pharmaceuticals, particularly antibiotics were carried out.[1–4]

Amoxicillin (AMX), a β-lactam antibiotic with bactericidal activity is used to treat many different types of infection, has a significant use in human health and veterinary treatments and is a potential pollutant in water.[5] The typical oral administration is 500 or 1000 mg as pills with a slow rate of metabolism in humans. For example, a dosage 500 mg of AMX in humans has led to an excretion of 87% in the urine after two hours of consumption.[6] Due to the complexity of AMX molecule is difficult to degrade completely. The kinetic disposition and biodistribution of AMX molecule were studied in mammals and birds. It was found that for buffalo calves[7] amoxicillin was distributed rapidly in various body tissues (kidney, liver, spleen, heart) and fluids (bile, urine) with concentrations higher than 5 μg/g or mL at 0.25 and 3 h after dosing. Appreciable levels of AMX were also assayed in the interstitial fluid from 1 to 4 h after drug administration, with a peak concentration of 6.7 + 0.3 μg/mL at 2 h. The AMX life-time depends on body mass, and for mammals and birds was found that AMX half-life increases with body mass raised.[8] For humans AMX have a plasma half-life of approximately 1.5 h and undergo little metabolism. During the first 6 h, 60–70% of an oral and 70–80% of an intravenous dose of AMX are recovered in the urine as unchanged drug.[9] However, AMX is unstable in aqueous solution and are known to undergo acid and base catalysed degradation to their 5R, 6R penicilloic acids, which then readily epimerize to the 5 S, 6R penicilloic acids under acidic and basic conditions. Other degradation products include the diketopiperazines and the dimers. All that compounds have been detected in biofluids and reported as metabolites of AMX.[9]

The usual methods used for the degradation of AMX in water matrices are the advanced oxidation processes based on photocatalytic methods,[10–11] Fenton/photo-Fenton,[10,12, 13] ozonation,[14] UV/H_2O_2[15] or by non-thermal plasma treatment.[16] All these oxidation methods involve drastic experimental conditions as lower pH, strong oxidants and/or apparatus conditions.

The electrochemical technologies have gained interested in water treatment and anodic oxidation may constitute a promising alternative to existing oxidation methods considering that it could provide an efficient oxidation in environmentally friendly conditions.[17–21] Electrochemical processes, which avoid the use of harmful redox agents, can provide valuable contributions to the protection of the environment through their implementation in wastewater treatment plants

[a] *M. Ferreira, Dr. I. Kuzniarska-Biernacka, Prof. Dr. A. M. Fonseca, Prof. Dr. I. C. Neves, Prof. Dr. P. Parpot*
Centro de Química CQUM
Campus de Gualtar
Universidade do Minho
Braga 4710-057 (Portugal)
E-mail: parpot@quimica.uminho.pt
[b] *Prof. Dr. A. M. Fonseca, Prof. Dr. I. C. Neves, Prof. Dr. P. Parpot*
Centre of Biological Engineering CEB
Campus de Gualtar
Universidade do Minho
Braga 4710-057 (Portugal)
[c] *Dr. O. S. G. P. Soares, Prof. Dr. M. F. R. Pereira, Prof. Dr. J. L. Figueiredo*
Laboratório de Catálise e Materiais LCM
Laboratório Associado LSRE/LCM
Universidade do Porto
Porto 4200-465 (Portugal)

Supporting information for this article is available on the WWW under https://doi.org/10.1002/cctc.201801193This manuscript i spart of Virtual Special Issue on the "Portuguese Conference on Catalysis" based on the International Symposium on Synthesis and Catalysis (ISySyCat).

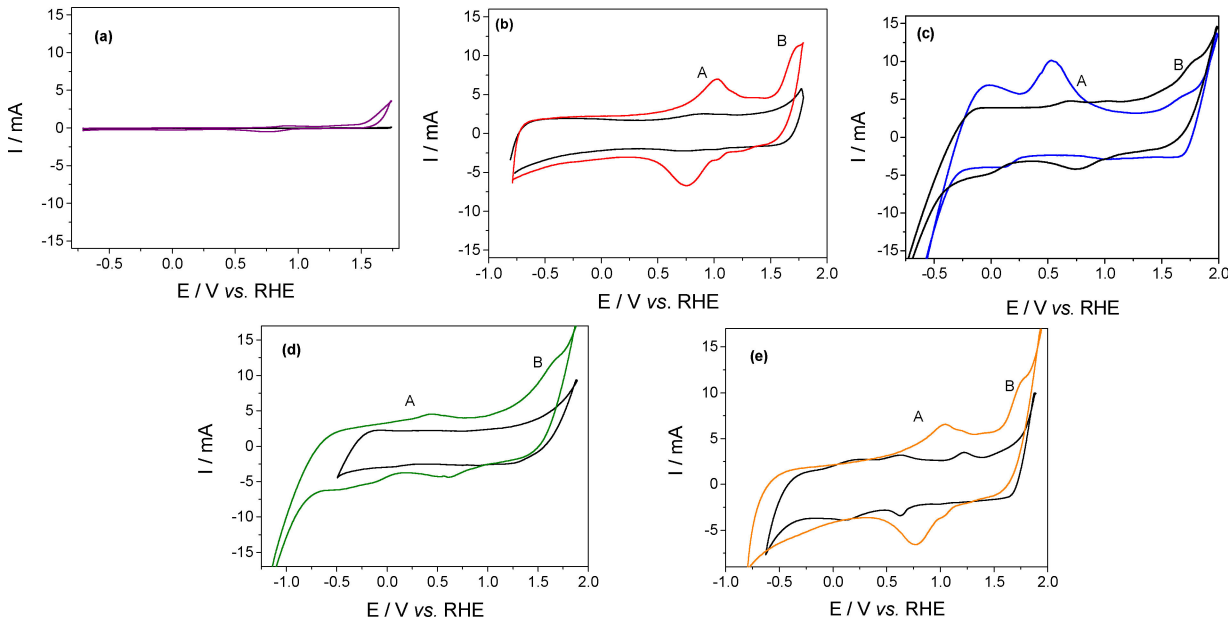

Figure 1. Cyclic voltammograms of a) CT, b) CNT, c) Pt/CNT, d) Ru/CNT and e) Pd/CNT in 0.1 M NaCl medium (black) in absence and (color) in presence of 2 mM AMX. Scan rate = 50 mV s^{-1}.

thanks to their versatility, energy efficiency, cost effectiveness and facility for process automation.[17–21]

Carbon nanotubes (CNT) are excellent candidate for both electrocatalyst and support materials for anodic oxidation considering their high surface area and physical properties.[22–24] The metals (Pt, Pd, Ru) studied in this work are considered good catalysts for the oxidation of organic compounds in aqueous media.[23–26]

This work aims to study the electrochemical reactivity of AMX on different metal carbon nanotubes catalysts in aqueous media, in order to elucidate the effect of major experimental parameters on current densities and oxidation potentials, and to determine the kinetic parameters of the redox reactions.

Results and Discussion

The electroreactivity of amoxicillin (AMX) on different modified electrocatalysts in several pH media was investigated using cyclic voltammetry. Two parameters were considered for the electrocatalyst assessment. The first one, is the current density obtained from the oxidation of the amoxicillin which depends on the reaction kinetics and the second one, is the oxidation potential which is related to the easiness of the redox reactions.

The cyclic voltammetry study was performed using CNT, Pt/CNT, Ru/CNT and Pd/CNT modified electrodes in 0.1 M NaCl and carbonate buffer (pH 10) and 0.1 M NaOH media. The mechanical and chemical stability of the electrode materials was also checked by cyclic voltammetry. The successive cycles show that the shape of the voltammograms remained unchanged confirming the stability of the electrocatalytic materials.

Voltammetric study in 0.1 M NaCl. Cyclic voltammetry can provide important data on substrate-electrode surface interaction *vs.* potential relationships. The voltammograms of Carbon Toray (CT) and CNT, Pt/CNT, Ru/CNT and Pd/CNT modified CT electrodes in 0.1 M NaCl medium are present in Figure 1. The graphs were represented with the same y axis scale in order to make easier the comparison between electrodes. It could be confirmed from these data that the oxidation current of AMX on CT electrode, which was the support material for the modified electrodes, is very low in comparison with that obtained for CNT or M/CNT electrodes.

In the presence of AMX in 0.1 M NaCl medium, two oxidation processes were noticed, the first one between 0.5 and 1.0 V *vs.* RHE (peak A), and the second one between 1.2 and 1.6 V *vs.* RHE (peak or "shoulder" B). The redox process observed for the unmodified CNT electrode confirms the interaction between electroactive species and the carbon surface, necessary for further oxidation. CNT and Pd/CNT electrodes show quite similar behavior with a well-defined redox process at 0.8/0.9 V *vs.* RHE (peak A). The phenolic group of AMX (Scheme 1) probably plays an important role in this case leading to phenoxy radical formation. These results are in agreement with those obtained by Kumar *et al.*[19] on MWNT/GCE electrode. Polymerization due to the accumulation of phenoxy radicals on the electrode surface could be reduced using diluted solutions and pH > 7. Nevertheless, the effect of the eventual polymerization on electrode response was not

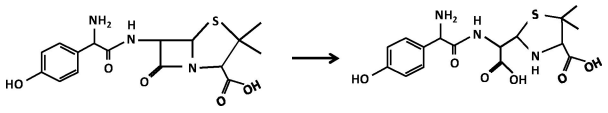

Scheme 1. Formation of penicilloic acid (APcA).

noticed in this case since the peak current intensities for successive cycles remained almost constant.

AMX molecule which has pKa values of 3.23 and 7.43 may have positive and negative charges corresponding respectively to the carboxylate anion and tertiary ammonium ion, in this pH medium. This configuration confers to the molecule the possibility of interacting with the electrode surface through several polar and non-polar parts. In this context, the approach of the benzene ring moiety to the carbon nanotubes and the subsequent adsorption of carbon atoms of carbonyl groups on the metal surface involving dehydrogenation may be envisaged. The AMX oxidation at Pt/CNT and Pd/CNT modified electrodes takes place in the potential region were the metal is partially oxidized. This can be explained by the strong CO adsorption on metal active sites in the potential region between −0.5 and 0.5 V *vs.* RHE for these modified electrocatalysts.

The formation of CO as poison species is probably due to the dehydrogenation of the molecule in hydrogen adsorption region followed by a dissociative adsorption. The decrease of the current intensities in the hydrogen region of platinum in the presence of AMX confirms the adsorption of this compound on the electrode surface in this potential region.

The expansion of oxidation currents starts with low oxygen coverage, sufficient for CO oxidation and becomes more important with higher amounts of adsorbed oxygenated species. The current intensity observed for peak B, in potential range from 1.2 to 1.6 V *vs.* RHE is probably due to the further oxidation of primary products; thus, this increase can be attributed to the ability of oxygen to concentrate these products by reactively scavenging them.[27]

The electroactivity of AMX on Pd/CNT is slightly better than that observed for the Pt electrocatalyst. This result is expected since palladium does not suffer as drastically from poisoning as does platinum. The oxidation of AMX on Ru_CNT starts at lower potentials than those observed for Pt/CNT and Pd/CNT electrocatalysts. Ru is apparently unique among the elemental electrode materials, considering its ability to oxidize CO_{ads} at low potentials *eg* below 0.4 V *vs.* RHE.[27] Polycrystalline Ru is covered with hydroxyl ions from water very early in the potential scale even in acidic solutions. Ru surface atoms, besides the sites for the dehydrogenation of AMX in an early stage of oxidation, can provide active sites for the adsorption of the oxygen-containing species at lower potentials. The further oxidation of adsorbed CO can occur as a surface reaction as represented in Equations (1) and (2):

$$Ru + H_2O \leftrightarrows (OH)_{ads} + H^+ + e^- \quad (1)$$

$$(CO)_{ads} + (OH)_{ads} \leftrightarrows CO_2 + H^+ + e^- \quad (2)$$

Ru can be used for modification of the platinum electrode with the aim of adsorbing oxygenated species in order to make the poison oxidation easier. However, too many oxygen species accumulated on the electrode surface may decrease the reaction rate even at high anodic potentials, since the adsorption of the organic substrate could be less efficient. In this context, the modification of CNT with a low amount of metal (M/CNT) could be useful, once the interaction of the molecule with the carbon surface and the restriction against the excess of M-oxygen species on the surface could be achieved.

In NaCl medium, low valence Ru species like $RuCl_3$ or $Ru(OH)_3$, produced on the electrode surface from 0.2 V *vs.* RHE, can act as redox agent in order to provide RuO_x species. The redox couple RuO_{x+1}/RuO_x acts as a mediator for the oxidation of organic compounds (potential range B) [Equation (3)]:

$$RuO_{x+1} + R \rightarrow RuO_x + RO \rightarrow \text{oxidation products} \quad (3)$$

Chlorine production on the electrode surface could be also foreseen in NaCl medium. Ru and RuO_2 are considered suitable for the production of active chlorine compounds on the electrode surface, since they can provide lower and higher over-potentials for chorine and oxygen production respectively, in comparison with other metals or carbonaceous electrodes.

Bimetallic catalyst composed of platinum and another element of group I b of the periodic table have been widely studied[22] with the aim of reducing the poison effect on the catalyst surface. Copper (Cu) is one of the more studied elements for this purpose considering its ability to adsorb oxygen containing compounds even at lower potentials. The cyclic voltammograms of Pt/Cu modified electrode in 0.1 M NaCl medium with and without AMX are given in Figure 2.

As expected an increase of the current intensities for the lower potential range was noticed for the bimetallic Pt/Cu catalyst, in comparison with those obtained on monometallic modified electrodes (see Figure 1). These results show that the deactivation of the Pt electrode can be decreased by the deposition of a second metal like Cu, since the second metal weakens the Pt–C bond, therefore increasing CO tolerance.

Voltammetric study in carbonate buffer (pH 10). Figure 3 shows the voltammograms of CT and CNT, Pt/CNT, Ru/CNT and Pd/CNT modified CT electrodes in carbonate buffer medium (pH 10). The maximum oxidation current densities of AMX for all these electrodes are in the same order of magnitude with the exception of CT electrode which exhibits very low oxidation currents in comparison with CNT or M/CNT modified electrodes.

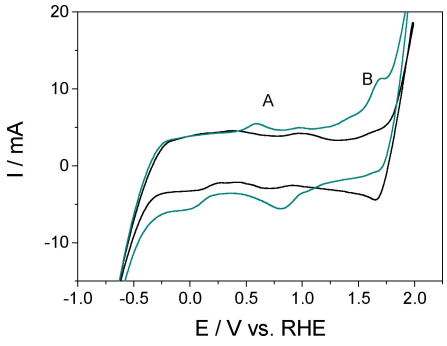

Figure 2. Cyclic voltammograms of Pt/Cu, in 0.1 M NaCl medium (black) in absence and (color) in presence of 2 mM AMX. Scan rate = 50 mV s^{-1}.

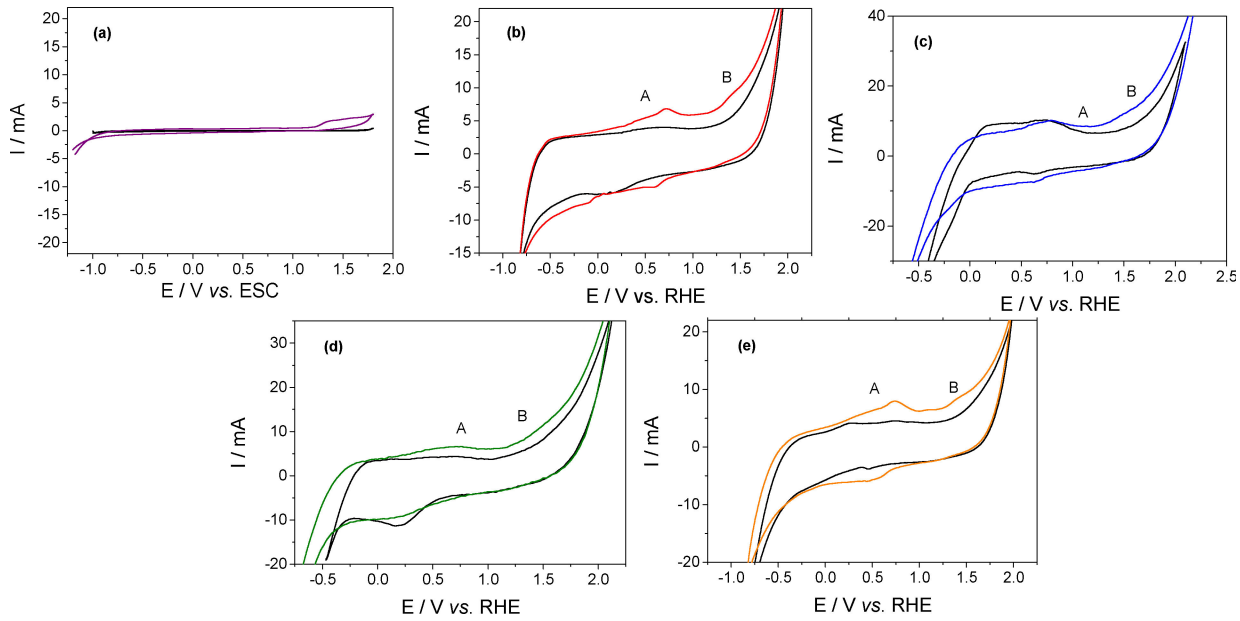

Figure 3. Cyclic voltammograms of a) CT, b) CNT, c) Pt/CNT, d) Ru/CNT and e) Pd/CNT in 0.1 M $NaHCO_3/Na_2CO_3$ buffer medium (black) in absence and (color) in presence of 2 mM AMX. Scan rate = 50 mV s^{-1}.

In alkaline medium (pH > 8), the carboxylic acid group of AMX is negatively charged (Scheme 1). Therefore, weaker interactions between the AMX molecule and the electrode surface than those observed for 0.1 M NaCl medium could be expected in this case due to the higher coverage of the oxygenated species on the electrode surface, in this case weaker interactions between the AMX molecule and the electrode surface than those observed for 0.1 M NaCl medium could be expected. This suggestion is in agreement with electrochemical data presented in Table 1 which indicates that an increase of pH provokes an important decrease for the peak A, while minor decreases are observed for peak B, which also depends on oxygen species on the electrode surface.

In alkaline media the following reaction steps can be considered for platinum modified electrode [Equations (4) to (8)]:

Table 1. Maximum current intensities and oxidation potentials for CNT, Pt/CNT, Ru/CNT, Pd/CNT electrodes in different supporting electrolytes.

Electrode	Supporting electrolyte	Current density Peak A [J_{ox}/mA mg^{-1}]	Current density Peak B [J_{ox}/mA mg^{-1}]
CNT	0.1 M NaCl	2.10	2.80
CNT	$NaHCO_3/Na_2CO_3$	1.26	1.60
CNT	0.1 M NaOH	1.20	1.90
Pt/CNT	0.1 M NaCl	0.70	2.20
Pt/CNT	$NaHCO_3/Na_2CO_3$	0.60	2.60
Pt/CNT	0.1 M NaOH	0.12	1.80
Ru/CNT	0.1 M NaCl	1.45	2.80
Ru/CNT	$NaHCO_3/Na_2CO_3$	1.10	2.50
Ru/CNT	0.1 M NaOH	0.65	2.10
Pd/CNT	0.1 M NaCl	2.02	2.60
Pd/CNT	$NaHCO_3/Na_2CO_3$	1.60	1.60
Pd/CNT	0.1 M NaOH	0.90	1.50

$$Pt + (R{-}HC(R'){-}R') \leftrightarrows Pt{-}(R{-}C(R''){-}R')_{ads} + H_{ads} \quad (4)$$

$$Pt + OH^- \leftrightarrows Pt{-}OH_{ads} + e^- \quad (5)$$

$$Pt{-}(R{-}C(R''){-}R')_{ads} + Pt{-}OH_{ads} + OH^- \leftrightarrows Pt{-}(R{-}C(OH){-}R') + R''OH + Pt \quad (6)$$

$$Pt{-}(R{-}C(OH){-}R') + OH^- \leftrightarrows Pt + (R{-}(CO){-}R') + H_2O + e^- \quad (7)$$

$$(R{-}(CO){-}R') + Pt{-}OH_{ads} + OH^- \leftrightarrows Pt + R{-}COOH + R'OH \quad (8)$$

Voltammetric study in 0.1 M NaOH. The 0.1 M NaOH medium does not provide a significant increase in overall current intensities of AMX oxidation on CNT/CT, Pt/CNT, Ru/CNT and Pd/CNT electrodes (Figure 4). Nevertheless, there are some differences especially for Pt and Pd electrodes considering the shape of the voltammograms, probably due to higher coverage of electrode surface by oxygenated species even at lower potentials. No oxidation occurs in this medium on CT electrode without modification.

In the 0.1 M NaOH medium opening of the β-lactam ring of AMX led to the formation of penicilloic acid (APcA)[11] providing a structure with two negative charges (Scheme 1):

An increase of the negatively charged regions may privilege the interaction between the carbon atom of the carbonyl group and the oxygen species adsorbed on the catalyst surface considering the susceptibility of a nucleophilic attack to the carbonyl group.

The voltammograms of the Pt electrode in 0.1 M NaOH before and after the addition of 2 mM AMX show no significant differences in the hydrogen region indicating that the adsorption of AMX takes place to a lower extent in this potential range than that noticed for the 0.1 M NaCl medium. In this pH

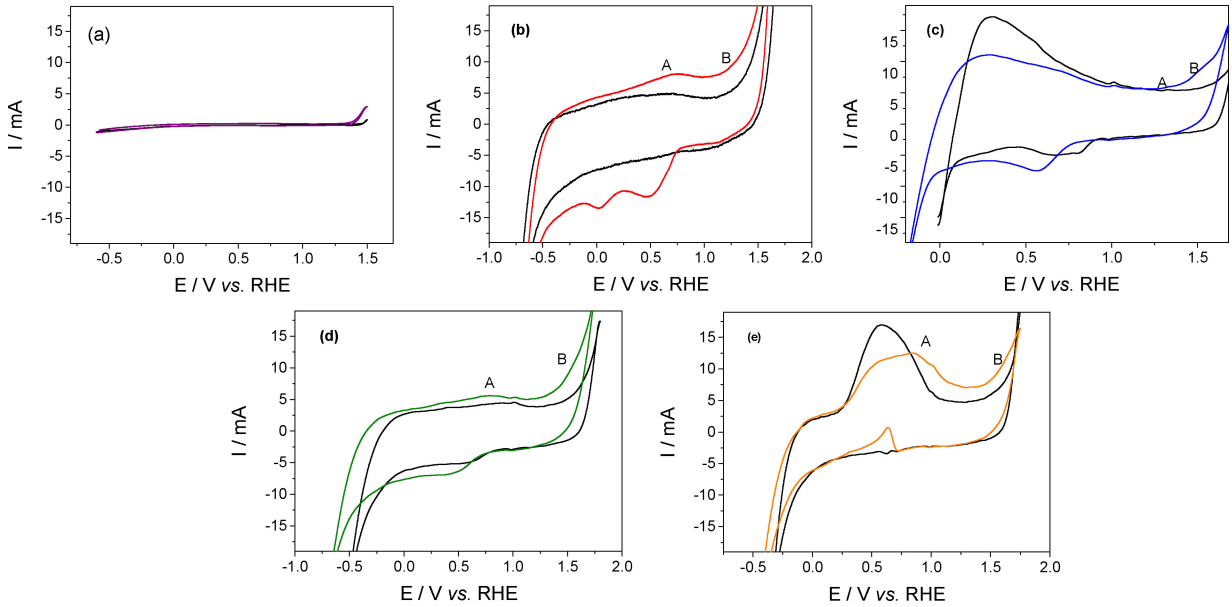

Figure 4. Cyclic voltammograms of a) CT, b) CNT, c) Pt/CNT, d) Ru/CNT and e) Pd/CNT in 0.1 M NaOH medium (black) in absence and (color) in presence of 2 mM AMX. Scan rate = 50 mV s^{-1}.

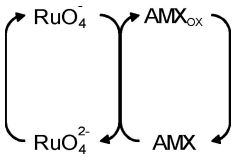

Scheme 2. Ru mediated oxidation pathways for AMX oxidation

medium, the formation of hydrates (diols) from carbonyl group and following interaction of -$C(OH)_2$ groups with adsorbed hydroxyl groups can be considered [Equations (9) to (11)]:

$$Pt + OH^- \leftrightarrows Pt{-}OH_{ads} + e^- \quad (9)$$

$$R\text{-}CO{-}R' + H_2O \leftrightarrows R{-}C(OH)_2{-}R' \quad (10)$$

$$R{-}C(OH)_2{-}R' + Pt{-}OH_{ads} + OH^- \leftrightarrows Pt + R{-}COOH + R'{-}OH + H_2O \quad (11)$$

Concerning the oxidation on the Ru modified electrode, $Ru(OH)_3$ species formed at potentials < 0.2 V *vs.* RHE can provide Ru(IV) oxides (RuO_2) according to the reactions [Equations (12) and (13):

$$Ru + 3H_2O \leftrightarrows Ru(OH)_3 + 3H^+ + 3e^- \quad (12)$$

$$Ru(OH)_3 + OH^- \leftrightarrows RuO_2 + 2H_2O \quad (13)$$

Further oxidation of RuO_2 gives Ru(VII) and Ru(VI) species which act as mediator for the oxidation of AMX as follows (Scheme 2):

A Pt/CNT electrocatalyst with higher platinum content (5 wt%) was prepared and tested in the same experimental conditions, in order to evaluate the effect of platinum loading on the electrocatalytic activity. The cyclic voltammograms of

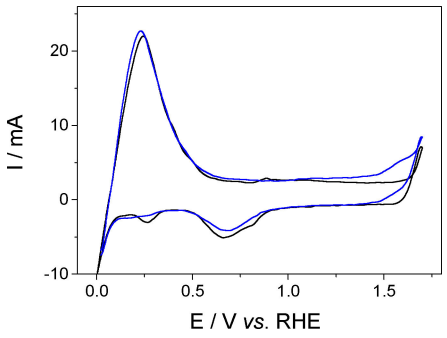

Figure 5. Cyclic voltammograms of Pt/CNT (5 wt% Pt) in 0.1 M NaOH medium (black) in absence and (color) in presence of 2 mM AMX. Scan rate = 50 mV s^{-1}.

the electrocatalyst with higher amount of Pt, in presence and absence of 2 mM AMX, are given in Figure 5.

The cyclic voltammogram of the electrocatalyst prepared with higher platinum content exhibit smooth platinum-like behavior in 0.1 M NaOH medium without AMX, as expected but did not provide higher current intensities for AMX oxidation than those observed for the Pt/CNT electrocatalyst with 1 wt% of Pt. This result shows that the factor which limits the reaction rate in this case could be the lack of the interactions between the hydrophobic parts of the molecule and carbon surface.

The electrochemical data obtained for different electrodes and supporting electrolytes are presented in Table 1. The standard deviation was below 5% for all the current densities.

The cyclic voltammogram of the electrocatalyst prepared with higher platinum content exhibit smooth platinum-like behavior in 0.1 M NaOH medium without AMX, as expected but did not provide higher current intensities for AMX oxidation than those observed for the Pt/CNT electrocatalyst with 1 wt% of Pt. This result shows that the factor which limits the reaction

Table 3. Maximum current intensities and initial oxidation potentials for the electrochemical oxidation of AMX on Pt/CNT, Ru/CNT and Pd/CNT modified electrodes in several pH media.

Electrode	pH	$I_{max.}$ Peak A [mA]	$I_{max.}$ Peak B [mA]	$E_{init.}$/V *vs.* RHE
−1 (Pt/CNT)	−1	0.70	2.20	0.84
−1 (Pt/CNT)	0	0.60	2.60	0.70
−1 (Pt/CNT)	1	0.12	1.80	1.44
0 (Ru/CNT)	−1	1.45	2.80	-0.11
0 (Ru/CNT)	0	1.10	2.50	0.09
0 (Ru/CNT)	1	0.65	2.10	0.26
1 (Pd/CNT)	−1	2.02	2.60	0.34
1 (Pd/CNT)	0	1.60	1.60	0.23
1 (Pd/CNT)	1	0.90	1.50	0.83
−1 (Pt/CNT)	−1	0.80	1.70	0.99
0 (Ru/CNT)	−1	1.28	2.40	0.07

rate in this case could be the lack of the interactions between the hydrophobic parts of the molecule and carbon surface.

Scan rate effect. Kinetic parameters of the reactions were determined using the scan rate study in 0.1 M NaCl, 0.1 M Na_2CO_3/$NaHCO_3$ buffer and 0.1 M NaOH, for peak A. The slopes of the logarithm of current density (j/mA mg^{-1}) *vs.* logarithm of scan rate (v/mV s^{-1}) provide information about the limiting step of the reaction, slopes of 0.5 and 1.0 corresponding to kinetics controlled by diffusion and adsorption steps (Table 2) respectively while the oxidation potential (E/V *vs.* RHE) vs. logarithm of (v/mV s^{-1}) allows to determine the reversibility of the processes. For Ru/CNT catalyst, the reaction corresponding to peak A is limited by the adsorption step in 0.1 M NaCl and by both adsorption and diffusion steps in 0.1 M Na_2CO_3/$NaHCO_3$ buffer and 0.1 M NaOH media, whereas for Pt and Pd electrocatalysts the diffusion step has a more significant contribution. This could be explained by the easier adsorption of the molecule in these last two cases.

These results show that the adsorption of the AMX molecule on Ru is more difficult to achieve than that observed for Pt and Pd modified electrodes. These results are in agreement with the previous suggestion based on the fast adsorption of the electroactive species on Pt and Pd sites. The dependence of the oxidation potential on the logarithm of the scan rate shows that the process is irreversible.

Table 2. Kinetic parameters of the oxidation reaction of amoxicillin in 0.1 M NaCl, 0.1 M carbonate buffer and 0.1 M NaOH on Pd/CNT, Pd/CNT and Ru/CNT modified electrodes.

Electrode	Supporting Electrolyte [0.1 M]	Potential range [mV]	Slope	Limiting step
Pt/CNT	NaCl	10-500	0.61	Diffusion
Ru/CNT	NaCl	10-500	0.93	Adsorption
Pd/CNT	NaCl	10-500	0.56	Diffusion
Pt/CNT	Na2CO3/NaHCO3	10-500	0.44	Diffusion
Ru/CNT	Na2CO3/NaHCO3	10-500	0.74	mixed
Pd/CNT	Na2CO3/NaHCO3	10-500	0.42	Diffusion
Pt/CNT	NaOH	10 - 250	0.40	Diffusion
Ru/CNT	NaOH	10-500	0.84	mixed
Pd/CNT	NaOH	10-500	0.39	Diffusion

Response surface strategy. The response surface graphs were prepared from the data presented in Table 3 using the design of experiments (DOE) methodology, in order to elucidate the importance of the different parameters and to determine the optimum experimental conditions for an efficient oxidation. Software packages, R (ver. 2.15.1) and Origin (ver. 7.5 from *OriginLab*), were used for this purpose.

In order to evaluate the effect of the electrode material and pH on maximum oxidation current intensities (peak A and B) and lowest oxidation potentials, the following matrix (Table 3) was used where Pt/CNT, Ru/CNT, Pd/CNT and 0.1 M NaCl, carbonate buffer (pH 10), 0.1 M NaOH correspond respectively to levels −1, 0, 1 for both electrode material and pH factors. For a more comprehensible comparison the potential values are given *versus* reference hydrogen electrode (RHE).

Effect of experimental parameters on current density. For I = f(electrode material; pH) relationships full factorial experimental design with two factors and tree levels was considered using the following model [Equation (14)]:

$$y = b_0 + b_1x_1 + b_2x_2 + b_{11}x_1^2 + b_{22}x_2^2 + b_{12}x_1x_2 \quad (14)$$

The number of experiments including 4 replicates was: $N = 3^2 + 4 = 13$. The correlation coefficient, F test for regression (F_{REG}) and for Lock of Fit (F_{LOF}) were respectively: 0.99 (peak A) and 0.95 (peak B); 119.0 (F_{REG}-peak A), 3.97 (F_{REG}-peak B); 0.98 (F_{LOF}-peak A) and 2.86 (F_{LOF}-peak B). These data show that the model is adequate since p-values for F_{REG} and F_{LOF} were respectively 1.06×10^{-6} (F_{REG}-peak A), 0.05 (F_{REG}-peak B) and 0.49 (F_{LOF}-peak A), 0.17 (F_{LOF}-peak B).[28] Surface and contour graphs for current density versus electrode material and pH relationships are presented in Figure 6.

Response value regions separated with circles and semi-circles with different diameters in contour graph and curvature observed, in response surface map and in surface graph show a second order effect. Nevertheless, this effect should not be very important once the corresponding p-values related to pure quadratic term for peak A and B are superior to 0.05: 0.10 and 0.28, respectively.

The ridge inclination of the surface map (surface graph) and semi-circles (contour graph) indicate an effect of interaction between modified electrode catalyst and pH for peak A. p-values for interactive term confirm this suggestion since they correspond to a significant level of 99.2% ($p = 0.00756$). Both the effect of electrode material and pH are important in this case corresponding significance levels superior to 95%. The statistical data show that for peak B, the factor electrode material and the interactive term are not significant since the obtained p-values are higher than 0.05. For the oxidation process corresponding to peak A both electrocatalyst and pH are important, while for peak B the only significant factor is pH. It can be also concluded that for the first peak (A) the effect of electrocatalyst is more important at lower pH media than what observed for higher pH. The highest current intensities correspond to Pd/CNT electrode in this case.

Considering that the surface deactivation, due to the irreversibly adsorbed CO is higher in neutral medium than in

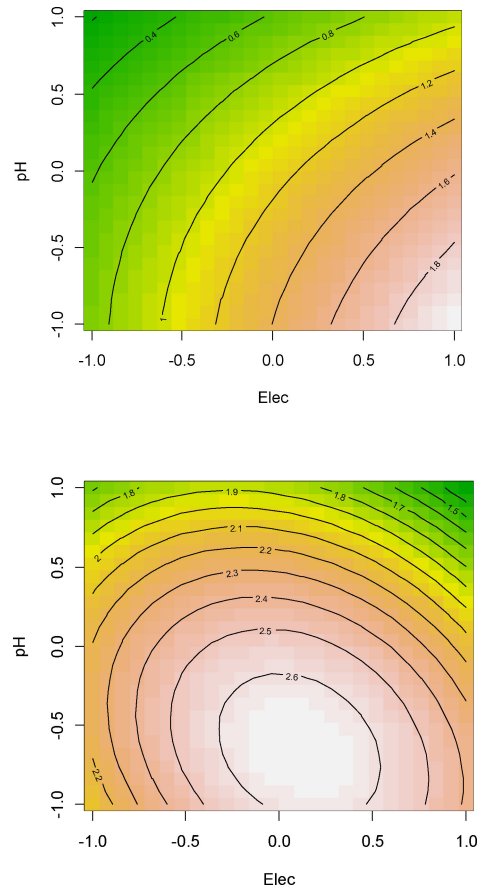

Figure 6. Contour graphs of Peak A (a) and Peak B (b) for current intensities *vs.* electrode material and pH relationships.

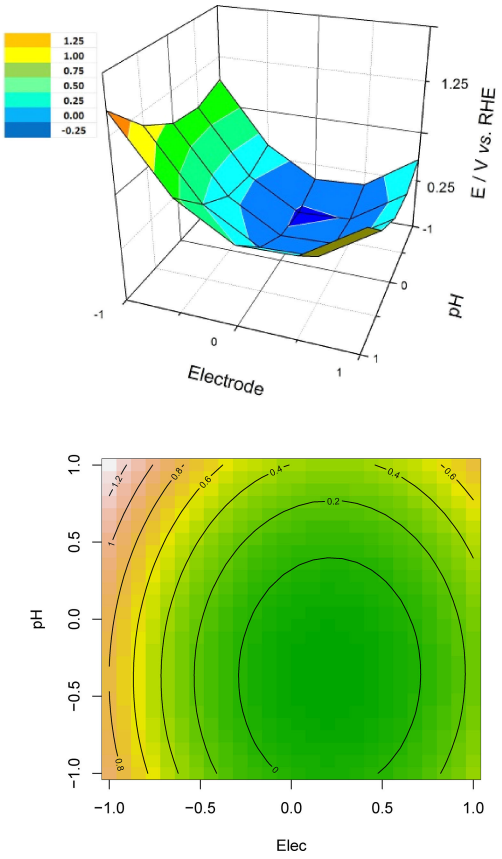

Figure 7. Surface (top) and contour graphs (bottom) for initial oxidation potential *vs.* electrode material and pH relationships obtained from full factorial experimental design strategy.

alkaline media these results are in agreement with the suggestions presented in the previous section. For the second peak, alkaline pH media and Ru/CNT electrode provides higher intensities. These results confirm the hypothesis that the adsorption of the molecule and related surface properties of the electrode material are more important for the first process than for the second one, which is more related to the oxygenated surface species and, consequently, to the OH^- ion concentration.

Effect of experimental parameters on oxidation potential. Full factorial design with the quadratic model given in equation 14 was used to elucidate the relationships between oxidation potential and two factors: electrode material and pH. The model could be considered adequate since the correlation coefficient. F_{REG} and F_{LOF} are respectively 0.98, 33.05 and 3.56 corresponding p-values of 1.0×10^{-4} and 0.13 for F_{REG} and F_{LOF} in this case (Figure 7).

The lack of the ridge for the response regions separated by circles show that there is no significant interaction effect between factors in this case while strong quadratic effect is observed. For quadratic and interactive terms, the p-values are respectively 0.83 and 1.4×10^{-4}. Both electrocatalyst and pH effect are significant with p-values of 6.5×10^{-5} and 1.9×10^{-3}, respectively. These results also show that on ruthenium modified electrocatalyst the oxidation starts at lower potentials in comparison with the other metallic electrocatalysts used in this work.

Optimization for an efficient oxidation. In order to determine the optimum conditions regarding to highest current intensities and lowest initial oxidation potentials, two surface were overlapped in the same graph and given in Figure 8.

It can be concluded from these graphs that there is no significant difference between the current intensities for peak A and for pH > 8, while an alkaline medium (pH = 10) provides higher intensities for peak B. For all pH media studied in this work, Ru provides the lowest potentials corresponding to the beginning of the AMX oxidation.

Considering that a suitable electrocatalyst should provide low oxidation potentials and significant current densities the Ru/CNT electrocatalyst could be a suitable choice for the efficient oxidation of AMX, since it satisfies this compromise.

Electrolysis of amoxicillin at Ru/CNT in 0.1 M NaOH medium. The electrolysis was carried out on the Ru/CNT electrode using an anode dimension of 2 cm × 2 cm and an anodic compartment of 250 mL. AMX was oxidized at 2.5 V *vs.* RHE. in 0.1 M NaOH medium in order to avoid the deactivation of the electrode surface by poison species like CO, produced by oxidation reaction. Simultaneous oxygen production provides the cleaning of the electrode surface removing these irrever-

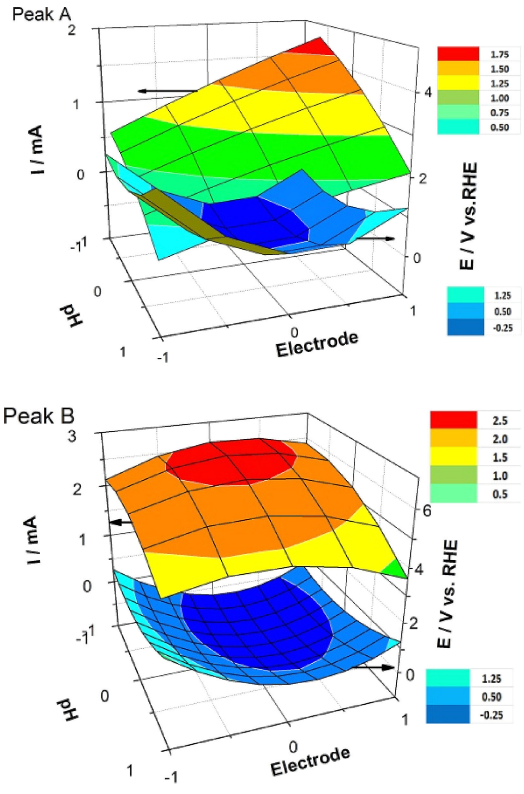

Figure 8. Surface graphs for $E_{initia}I$ and I_{max} *vs.* electrode material and pH relationships for peak A (top) and peak B (bottom).

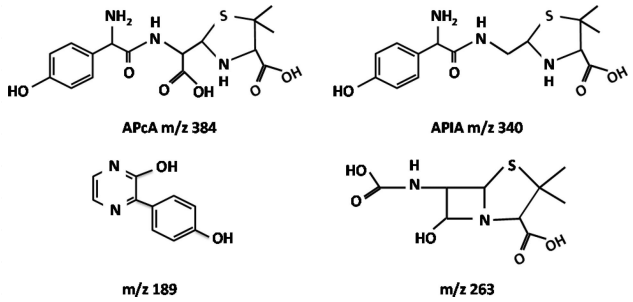

Figure 9. Oxidation products of amoxicillin identified by HPLC-MS.

sibly adsorbed species. After 8 h of electrolysis, the decrease of the initial AMX concentration reaches 45% while oxidation current intensities fallen from 0.19 A, at the beginning of the electrolysis, to 0.05 A at the end. The ln[AMX] *vs.* time curve shows a linear relationships indicating that the reaction was the first order with respect of AMX concentration. The rate constant, calculated from the slope value was 3.2×10^{-5} s^{-1}. Electrolysis products were analyzed by HPLC-MS and IC while the mineralization rate was determined by TOC analysis. HPLC-ESI (+)-MS analyses show the presence of two ions with significant abundance corresponding to m/z ratios of 189 and 263 among the oxidation products, besides the AMX, penicilloic (APcA) and penilloic (APIA) acids identified by ions with m/z 384, 367, 340 and 323.[29] These ions could be attributed

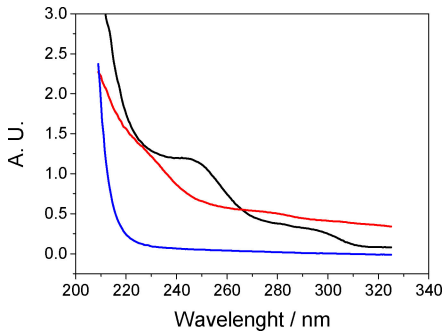

Figure 10. UV-Vis spectra of blank electrolysis solution (blue), AMX (black) and electrolyzed solution of AMX (red) on Ru/CNT modified electrode, in 0.1 M NaOH, at 2.5 V vs. RHE.

respectively to the phenyl hydroxypyrazine and C9-dicarboxylic acid given in Figure 9.

The relatively high abundance of these compounds among oxidation products indicates that an interaction between the carbon atom of the carbonyl group in hydrated or non-hydrated forms and oxygen species on electrode surface can be foreseen since this carbon atom, considering its charge distribution, is suitable for a nucleophilic attack by surface OH species (Scheme 3).

Formic acetic and propionic acids and CO_3^{2-} determined at the end of the electrolysis correspond to 7, 6, 9 and 26% of the oxidized AMX, respectively. The carbonate percentage, determined by IC, is in agreement with TOC results which indicate a mineralization of 28% for transformed AMX. Sulfate and nitrate concentrations in electrolyzed solution were respectively 0.15 and 0.12 mM, which corresponds to sulfur mineralization of 17% and nitrogen mineralization of 4%.

UV-Vis spectra of amoxicillin (2 mM) and electrolyzed solution of amoxicillin are given in Figure 10.

The decrease of absorbance in the region from 230 to 270 nm, attributed to the presence of amoxicillin shows the consumption of this compound during the electrolysis. This decrease also indicates that among the oxidation products the share of phenolic compounds did not correspond to high percentages since their absorption bands maxima are included in the same range of wavelengths.

No significant degradation of AMX was noticed in this medium, during the time period corresponding to that applied to the electrolysis since the decrease observed in the chromatographic peak area of AMX for the control experiments was less than 5%, (Figure S1 – supporting information).

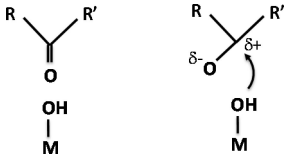

Scheme 3. Nucleophilic attack by surface OH species.

Conclusions

The electrochemical oxidation of the organic compounds involves either interaction of the substrate with surface OH groups generated at high potentials. or direct electron transfer from the organic molecule to the electrode. For an efficient anodic oxidation, a significant interaction between the electroactive species and the electrode surface is necessary in order to permit the fast adsorption of the molecule. But, on the other hand, the irreversible adsorption of the poison species like CO on the electrode surface must be avoided. Cyclic voltammetry study shows that two oxidation processes can be observed in presence of AMX: the first one corresponding probably to the dehydrogenative adsorption and further oxidation of AMX and the second one likely corresponds to the oxidation of primary products on a surface covered by oxygenated species. Concerning the current intensities involved in the first process (peak A), it seems that both the electrode material and pH have important effect while only the pH effect is significant for the second one. The electroreactivity study of AMX on Pt/CNT, Pd/CNT and Ru/CNT modified electrocatalysts in different pH media combined with experimental design strategy shows that Ru supported on CNT allows to satisfy the compromise concerning low anodic potentials and relatively high current intensities. The electrolysis of 2 mM AMX on Ru/CNT in 0.1 M NaOH medium and further HPLC, IC and HPLC-MS analyses of the reaction products let us to conclude about the oxidation reaction pathways.

Experimental Section

Materials and Reagents. The multiwalled carbon nanotubes (Nanocyl-3100) (CNT) samples and the metal precursors (H_2PtCl_6, $PdCl_2$, $RuCl_3$ and $Cu(NO_3)_2$) were purchased from Nanocyl and Alfa Aesar, respectively. The supporting electrolytes were prepared using ultrapure water (18 MΩ cm, Barnsted E-pure system) and sodium chloride (Panreac, 99.5%), sodium carbonate anhydrous (Panreac, 99.8%) and sodium bicarbonate (Panreac, 98%) were used without purification. Amoxicillin and HPLC standards were reagent grade and purchased from Sigma-Aldrich. Carbon Toray (CT) paper was obtained from Quintech.

Preparation of carbon nanotube supported metal catalysts. The active metals were supported on CNT. The monometallic/CNT (Pd, Ru and Pt) catalysts were prepared by the incipient wetness method and the bimetallic/CNT (Pt–Cu) catalyst by co-impregnation with aqueous solutions of the corresponding metal precursors in according to the methods describe in literature.[19–21] After impregnation, the catalysts were dried at 100 °C for 24 h and followed by heat treatment under nitrogen flow at 200 °C for 1 h and reduced at 200 °C under hydrogen flow for 3 h, with the exception of the Ru catalyst which was heat treated and reduced at 250 °C. A nitrogen flow was used during cooling to room temperature. The contents of noble metals and copper were kept always at 1.0 wt%. The catalyst samples were characterized using different techniques: temperature programmed reduction (TPR), transmission electron microscopy (TEM) and X-ray photoelectron spectroscopy (XPS), further details can be found in previous works.[30,31]

Preparation of carbon nanotube and metal-carbon nanotube modified electrodes. The preparation of the modified electrodes was performed by a previously established procedure described in our published works[19–21] from CNT or M/CNT suspensions in Nafion/water solution. After deposition of the electrocatalytic material on a Carbon Toray (CT) paper, this last one was glued to the platinum electrode using conductive carbon cement and dried at room temperature during 24 h. The cleanness of the surface was tested prior to each experiment by recording voltammograms in the supporting electrolyte medium alone.

Electrochemical Setup. The voltammetric study was performed in a thermostated three-electrode glass cell and a two-compartment glass cell separated by ion exchange membranes (Nafion 117 (Dupond de Nemours) and Ionac (Sybron Chemicals Inc.). The reference and counter electrodes were a saturated calomel electrode and platinum foil (99.95%) respectively. All the potentials are given *versus* reference hydrogen electrode (RHE) for easier comparison between different pH media. Ultra-pure nitrogen (U Quality from Air Liquide) was used to de-aerated the solutions and to maintain an inert atmosphere over the solutions during the measurements. The electrochemical instrumentation consisted of a potentiostat/galvanostat from Amel Instruments coupled to a computer by an AD/DA converter. The Labview software (National Instruments) and a PCI-MIO-16E-4 I/O module were used for generating and applying the potential program as well as acquiring data, such as current intensities.

Analytical Techniques for Product Analysis

Two chromatographic set-ups were used for the quantitative analysis of reaction products. The first one consisted of a high performance liquid chromatograph (HPLC) with an isocratic pump and double on-line detection including UV-Vis and refraction index detectors, and the second one an ion chromatography (IC, Dionex) with a conductivity detector. The separation of reaction products was carried out using Aminex HPX-87 H (Biorad) and Merck C18 analytical columns for HPLC-UV and AS11-HC column (Dionex Corp.) for IC. ESI-MS and HPLC-MS analyses were effectuated using Finnigan Survayor Chromatography system coupled to LxQ Thermo Mass Detector. The mobile phase was water with 0.1% acetic acid (solvent A) and acetonitrile (solvent B), at a flow rate of 0.3 mL/min. A linear gradient progressed from 10% B (initial conditions) to 90% B in 15 min and returned to the initial conditions after 5 min. The HPLC system was connected to a linear ion trap mass spectrometer with an electrospray interface operated under the following conditions: Mass spectra were acquired in a mass range of 50–500 amu). The instrument was operated in positive and negative ionization mode, with capillary voltage of 43 and −49 V, respectively for positive and negative ionization mode. The mass spectrometry data was handled using Excalibur software. TOC analyses were carried out by the NPOC method using a LTOC Total Organic Carbon Analyzer of Shimadzu coupled to an ASI–L auto sampler of the same brand.

Acknowledgements

The authors thank FCT (Fundação para a Ciência e a Tecnologia) for the PhD grant of Marta Ferreira. This work is also a result of project BioTecNorte (operation NORTE-01-0145-FEDER-000004) and AIProcMat@N2020 (operation NORTE-01-0145-FEDER-000006), supported by Norte Portugal Regional Operational Programme (NORTE 2020), under the Portugal 2020 Partnership Agreement through the European Regional Development Fund (ERDF). This work also has been funded by ERDF through

COMPETE2020 - Programa Operacional Competitividade e Internacionalização (POCI), POCI-01-0145-FEDER-006984 – Associate Laboratory LSRE-LCM, and by national funds through FCT for PTDC/AAGTEC/5269/2014 and Centre of Chemistry (UID/QUI/00686/2013 and UID/QUI/0686/2016).

Conflict of Interest

The authors declare no conflict of interest.

Keywords: Amoxicillin · electrochemical oxidation · electrocatalyst based on carbon nanotubes · surface *vs.* reactivity relationships

[1] J. C. G. Sousa. A. R. Ribeiro, M. O. Barbosa, M. F. R. Pereira, A. M. T. Silva, *J. Hazard. Mater.* **2018**, *344*, 146–162.
[2] D. Shahidi, R. Roy, A. Azzouz, *Appl. Catal. B* **2015**, *174*, 277–292.
[3] B. Silva, F. Costa, I. C. Neves, T. Tavares, In *Psychiatric Pharmaceuticals as Emerging Contaminants in Wastewater.* Springer Book. SpringerBriefs in Green Chemistry for Sustainability, **2015**, Vol. III. pp. 1–18.
[4] D. Fatta-Kassinos, S. Meric, A. Nikolaou, *Anal. Bioanal. Chem.* **2011**, *399*, 251–275.
[5] I. Gozlan, A Rotstein, D. Avisar, *Chemosphere.* **2013**, *91*, 985–992.
[6] A. F. Martins, F. Mayer, E. C. Confortin, C. D. Frank, *Clean.* **2009**, *37*, 365–371.
[7] H. N. Khanikor, A. K. Srivastava, B. S. Paul, Dr. J. K. Malik, *J. Vet. Med. Ser. A* **1986**, *33*, 212–218.
[8] L. D. Lashev, D. A. Pashov, *Res. Vet. Sci.* **1992**, *53*, 160–164.
[9] S. C. Connor, J. R. Everett, K. R. Jennings, J. K. Nlcholsont, G. Woodnutt, *J. Pharm. Pharmacol.* **1994**, *46*, 128–134.
[10] D. Klauson, J. Babkina, K. Stepanova, M. Krichevskaya, S. Preis, *Catal. Today.* **2010**, *151*, 39–45.
[11] D. Kanakaraju, J. Kockler, C. A. Motti, B. D. Glass, M. Oelgemoller, *Appl. Catal. B* **2015**, *166*, 45–55.
[12] A. G. Trovó, R. F. P. Nogueira, A. Agüera Amadeo, R. Fernandez-Alba, S. Malato, *Water Res.* **2011**, *45*, 1394–1402.
[13] E. S. Elmolla, M. Chaudhuri, *J. Hazard. Mater.* **2009**, *172*, 1476–1481.
[14] F. J. Benitez, J. L. Acero, F. J. Real, G. Roldán, *Chemosphere* **2009**, *77*, 53–59.
[15] Y. J. Jung, W. G. Kim, Y. Yoon, J.-W. Kang, Y. M. Hong, H. W. Kim, *Sci. Total Environ.* **2012**, *420*, 160–167.
[16] M. Magureanu, D. Piroi, N. B. Mandache, V. David, A. Medvedovici, C. Bradu, V. I. Parvulescu, *Water Res.* **2011**, *45*, 3407–3416.
[17] G. Chen, *Sep. Purif. Technol.* **2004**, *38*, 11–41.
[18] S. Ganiyu, N. Oturan, S. Raffy, M. Cretin, R. Esmilaire, E. Van Hullebusch, G. Esposito, M. A. Oturan, *Water Res.* **2016**, *106*, 171–182.
[19] A. S. Kumar, S. Sornambikai, L. Deepika, J.-M. Zen, *J. Mater. Chem.* **2010**, *20*, 10152–10158.
[20] Z. Frontistis, M. Antonopoulou, D. Venieri, I. Konstantinou, D. Mantzavinos, *J. Environ. Manage.* **2017**, *195*, 100–109.
[21] X. Zhao, Y. Hou, H. Liu, Z. Qiang, J. Qu, *Electrochim. Acta* **2009**, *54*, 4172–4179.
[22] M. Ferreira, M. F. Pinto, I. C. Neves, A. M. Fonseca, O. S. G. P. Soares, J. J. M. Órfão, M. F. R. Pereira, J. L. Figueiredo, P. Parpot, *Chem. Eng. J.* **2015**, *260*, 309–315.
[23] M. Ferreira, M. F. Pinto, O. S. G. P. Soares, M. F. R. Pereira, J. J. M. Órfão, J. L. Figueiredo, I. C. Neves, A. M. Fonseca, P. Parpot, *Chem. Eng. J.* **2013**, *228*, 374–380.
[24] M. Ferreira, M. F. Pinto, O. S. G. P. Soares, M. F. R. Pereira, J. J. M. Órfão, J. L. Figueiredo, I. C. Neves, A. M. Fonseca, P. Parpot, *Electrochim. Acta.* **2012**, *60*, 278–286.
[25] E. H. Yu, K. Scott, R. W. Reeve, *J. Electroanal. Chem.* **2003**, *547*, 17–24.
[26] L. Davidson, Y. Quinn, D. F. Steele, *Platinum Met. Rev.* **1998**, *42*, 90–97.
[27] J. Lipkowski, P. N. Ross, In *Electrocatalysis*, Wiley-VCH, New York, **1998**, pp 43–74.
[28] D. L. Massart, B. G. M. Vandeginste, S. M. Deming, Y. Michotte, L. Kaufman, In *Chemometrics: a textbook. Data Handling in Science and technology- vol. 2.* Elsevier. **2003**.
[29] E. Nägele, R. Moritz, *J. Am. Soc. Mass Spectrom.* **2005**, *16*, 1670–1676.
[30] O. S. G. P. Soares, J. J. M. Orfão, M. F. R. Pereira, *Ind. Eng. Chem. Res.* **2010**, *49*, 7183–7192.
[31] O. S. G. P. Soares, A. G. Gonçalves, J. J. Delgado, J. J. M. Órfão, M. F. R. Pereira, *Catal. Today*, **2015**, *249*, 199–203.

Manuscript received: July 23, 2018
Accepted Article published: August 31, 2018
Version of record online: October 9, 2018